NT-MDT
Spectrum Instruments

Scientific Digest

Confocal Raman Microscopy with NTEGRA Spectra

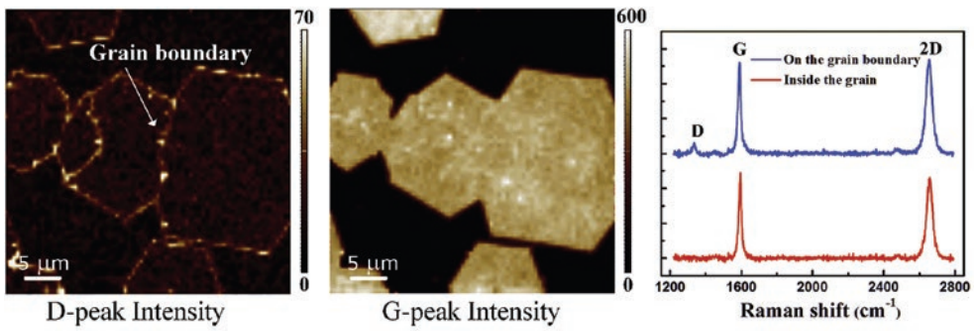

Integration of AFM with confocal Raman/fluorescence microscopy provides wide range of physical and chemical information about the sample. Simultaneously measured AFM and Raman maps of exactly the same sample area provide complementary information about sample physical properties (AFM) and chemical composition (Raman).

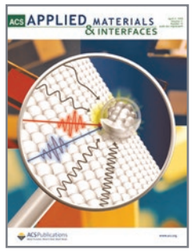

Wafer-Scale Substitutional Doping of Monolayer MoS_2 Films for High-Performance Optoelectronic Devices

Kim, Y., Bark, H., Kang, B., & Lee, C.
ACS Appl. Mater. Interfaces 2019, 11, 13, 12613–12621
https://doi.org/10.1021/acsami.8b20714

The substitutional doping method is ideally suited to generating doped two-dimensional (2D) materials for practical device applications as it does not damage or destabilize such materials. However, recently reported substitutional doping techniques for 2D materials have given rise to discontinuities and low uniformities, which hamper the extension of such techniques to large-scale production. In the current work, we demonstrated uniform substitutional doping of monolayer MoS_2 in a 2 in. wafer of area >13 cm^2. The devices based on doped MoS_2 showed extremely high uniformity and stability in electrical properties in ambient conditions for 30 days. The photodetectors based on the doped MoS_2 samples showed an ultrahigh photoresponsivity of 5×10^5 A/W, a detectivity of 5×10^{12} Jones, and a fast response rate of 5 ms than did those based on undoped MoS_2. This work showed the feasibility of real-life applications based on functionalized

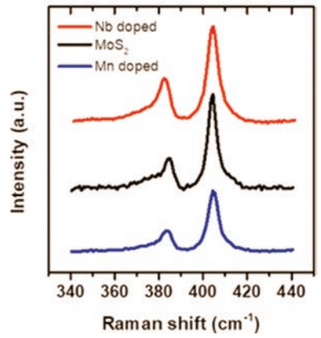

2D semiconductors for next-generation electronic and optoelectronic devices.

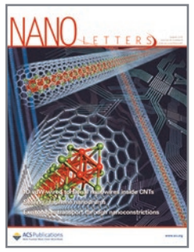

Nonlinear Raman Effects Enhanced by Surface Plasmon Excitation in Planar Refractory Nanoantennas

Sergey S. Kharintsev, Anton V. Kharitonov, Semion K. Saikin, Alexander M. Alekseev, and Sergei G. Kazarian
Nano Letters 2019, 19(8), 5017–5024
http://dx.doi.org/10.1021/acs.nanolett.7b02252

We consider a nonlinear mechanism of localized light inelastic scattering within nanopatterned plasmonic and Raman-active titanium nitride (TiN) thin films exposed to continuous-wave (cw) modest-power laser light. Owing to the strong third-order nonlinear interaction between optically excited broadband surface plasmons and localized Stokes and anti-Stokes waves, both stimulated and inverse Raman effects can be observed. We provide experimental evidence for coherent amplification of the localized Raman signals using a planar square-shaped refractory antenna.

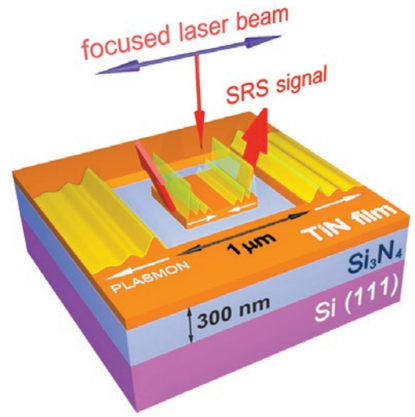

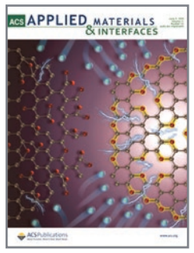

Encapsulation of a Monolayer WSe_2 Phototransistor with Hydrothermally Grown ZnO Nanorods

Kang-Nyeoung Lee, Seungho Bang, Ngoc Thanh Duong, Seok Joon Yun, Dae Young Park, Juchan Lee, Young Chul Choi, Mun Seok Jeong
ACS Appl. Mater. Interfaces 2019, 11, 20257−20264
https://doi.org/10.1021/acsami.9b03508

Transition metal dichalcogenides (TMDCs) are promising two-dimensional (2D) materials for realizing next-generation electronics and optoelectronics with attractive physical properties. However, monolayer TMDCs (^{1L}TMDCs) have various serious issues, such as instability under ambient conditions and low optical quantum yield from their extremely thin thickness of ~0.7 nm. To overcome these issues, we constructed a hybrid structure (HS) by growing zinc oxide nanorods (ZnO NRs) on a monolayer tungsten diselenide ($^{1L}WSe_2$) using the hydrothermal method. Consequently, we confirmed not only enhanced photoluminescence of $^{1L}WSe_2$ but also improved optoelectronic properties by fabricating the HS phototransistor. Through various investigations, we found that these phenomena were due to the antenna and p-type doping effects attributed to the ZnO NRs. In addition, we verified that the optoelectronic properties of 1LTMDCs are maintained for

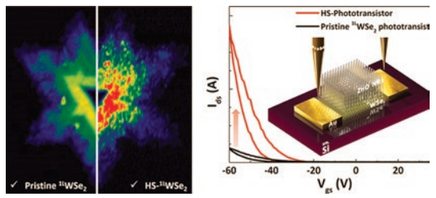

2 weeks in ambient condition through the sustainable encapsulation effect induced by our HS. This encapsulation method with inorganic materials is expected to be applied to improve the stability and performance of various emerging 2D material-based devices.

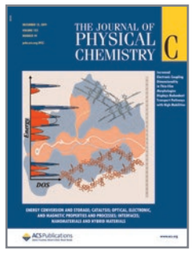

Insights into the Interaction of Graphene Oxide and Adsorbed RhB by Raman Spectral Deconvoluted Scanning

Berrellez-Reyes, F., & Alvarez-Garcia, S.
Journal of Physical Chemistry C 2019, 123(49), 30021–30027
https://doi.org/10.1021/acs.jpcc.9b09353

In this work, we study the interaction of a graphene oxide (GO) substrate and adsorbed rhodamine B (RhB) molecules by Raman spectral deconvoluted scanning. We achieved the deconvolution of a large number of spectra with overlapping Raman bands of GO and RhB. The evolution of the deconvolution parameters is shown as two-dimensional (2D) spatial maps, cross-correlation graphs, and evolution curves of the statistical representation derived from the data histogram. We show that at resonant excitation of the RhB molecules, the dye fluorescence is quenched, and the GO Raman bands are modified. We report a downshift in the G-band position and an increase in the intensity of the defect-activated D- and D′-band with a higher amount of adsorbed RhB molecules. These results will be discussed considering previously reported works on Raman spectra dependence with molecular-doped and gate-voltage-doped graphene.

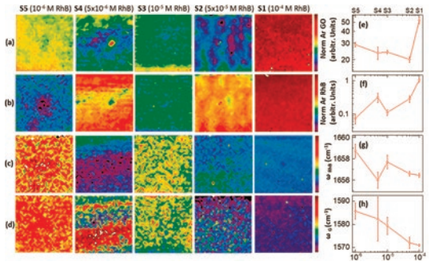

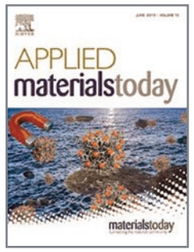

Mildly Oxidized SWCNT as New Potential Support Membrane Material for Effective H_2/CO_2 Separation

Boháčová, M., Zetková, K., Knotek, P., Bouša, D., Friess, K., Číhal, P., Lanč, M., Hrdlička, Z., & Sofer, Z.
Applied Materials Today 2019, 15, 335–342
https://doi.org/10.1016/j.apmt.2019.02.014

We demonstrate challenging material properties of flat free-standing chemically modified single wall carbon nanotube (SWCNT) sheets potentially usable as new support materials for gas separation composite membranes. Carbon nanotube samples in bare and oxidized forms were assembled into buckypaper by a vacuum filtration from SWCNT colloidal suspension. The fundamental structure, composition and mechanical properties were examined via SEM, EDS, AFM, XPS, Raman spectroscopy and dynamical mechanical analysis. Gas permeability was determined by the fixed-volume pressure-increase permeation method at 25 °C and 1 bar feed overpressure. The mild SWCNT oxidation caused substantial structural rearrangement of buckypaper with significant impact on its properties. Determined partial opening of nanotubes and the introduction of oxygen-containing species decreased the initial extremely-high H_2 permeability from circa 20 million (bare)

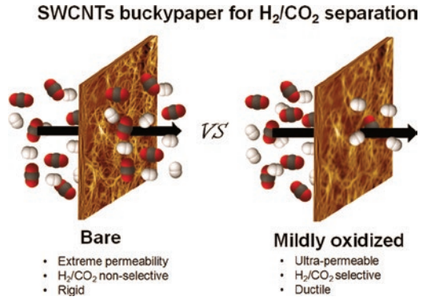

to almost 5 million barrers while the ideal H_2/CO_2 selectivity α increased from almost non-selective 1.1 (bare) to 3.5 for the oxidized sample.

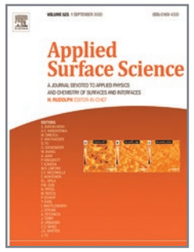

Ageing Effects at Graphene/Germanium Interface

Mendoza, C. D., Maia da Costa, M. E. H., & Freire, F. L.
Applied Surface Science 2019, 497, 143779
https://doi.org/10.1016/j.apsusc.2019.143779

X-ray photoelectron spectroscopy (XPS), atomic force microscopy (AFM), Raman spectroscopy and scanning tunnelling microscopy/spectroscopy (STM/STS) were used to study the effects of a long exposition to the air moisture of the interface between graphene and Ge (110) substrate. The single-layer graphene was grown by chemical vapour deposition (CVD) directly on Ge. The Raman and XPS results indicated that oxidation occurs slowly probably due to the diffusion of oxygen containing species through short-circuits like defects and grain boundaries present in the graphene sheet, as revealed by AFM and STM. In a long time-scale, the oxidation process resulted in a decoupling between graphene and germanium and a modification of the local density of states measured by STS.

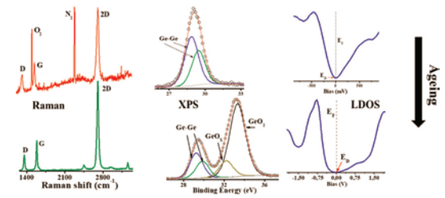

Chitosan Coatings Ionically Cross-Linked with Ammonium Paratungstate as Anticorrosive Coatings for Zinc

Szőke, Á. F., Szabó, G., Simó, Z., Hórvölgyi, Z., Albert, E., Végh, A. G., Zimányi, L., & Muresan, L. M.
European Polymer Journal 2019, 118(May), 205–212
https://doi.org/10.1016/j.eurpolymj.2019.05.057

Chitosan (Chit) coatings deposited on zinc by dip coating technique were impregnated with ammonium paratungstate (PTA) to improve their anticorrosive effect. UV–Vis spectroscopy was used to determine the layer thickness on glass substrates, while PTA accumulation and retention were studied on quartz. The behavior of the native and the PTA loaded chitosan coatings, along with their degradation in time were studied with Raman spectroscopy, EDS, AFM, potentiodynamic polarization and electrochemical impedance spectroscopy techniques. Impregnation has significantly lowered the swelling speed of chitosan, additionally, PTA has been retained in the coatings even after 3 days of exposure to a corrosive environment. The strong ionic cross-linking also improved corrosion inhibition effects (from 29% to 98%) of the chitosan coatings by decreasing the permeability of the layer. The Chit-PTA system can be successfully applied as a short-term anticorrosive

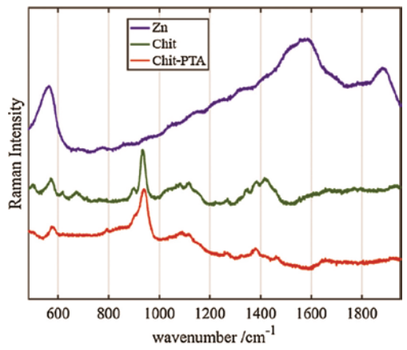

coating, removable on demand without damaging the underlying substrate.

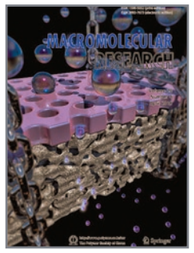

Preparation of Thin-Layer Graphene Using RAFT Polymerization and a Thiol-Ene Click Reaction

Minho Kwon, Taeheon Lee, Youngsil Lee, Jong Hun Han, Hyun-jong Paik
Macromolecular Research 2019, 27, 955–962
https://doi.org/10.1007/s13233-019-7201-6

In this paper, functionalization of graphene is conducted through click reactions for its effective dispersion. The poly(sodium 4-styrenesolfonate) (PSS) was synthesized using reversible addition-fragmentation chain transfer (RAFT) polymerization. The chain end dithioester group of RAFT-polymerized PSS was reduced to a thiol and used to couple PSS to graphene oxide (GO) via a thiol-ene click reaction. An aqueous dispersion of reduced GO with PSS (PSS-rGO) resisted sedimentation due to steric effects and charge-charge repulsion between the PSS attached to rGO. Atomic force microscopy showed that the PSS-rGO mixture was composed of dispersed particles of thin-layer (1.5 nm thick) graphene. Thickness of the PSS-rGO was close to that of GO. This indicates that there was no significant re-aggregation during GO reducing process.

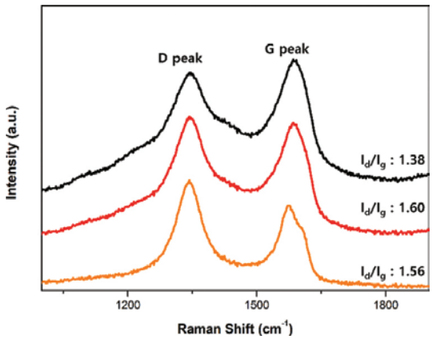

Influence of Chemical Fixation Process on Primary Mesenchymal Stem Cells Evidenced by Raman Spectroscopy

Lazarević, J. J., Ralević, U., Kukolj, T., Bugarski, D., Lazarević, N., Bugarski, B., & Popović, Z. V.
Spectrochimica Acta - Part A: Molecular and Biomolecular Spectroscopy 2019, 216, 173–178
https://doi.org/10.1016/j.saa.2019.03.012

In investigation of (patho)physiological processes, cells represent frequently used analyte as an exceptional source of information. However, spectroscopic analysis of live cells is still very seldom in clinics, as well as in research studies. Among others, the reasons are long acquisition time during which autolysis process is activated, necessity of specified technical equipment, and inability to perform analysis in a moment of sample preparation. Hence, an optimal method of preserving cells in the existing state is of extreme importance, having in mind that selection of fixative is cell lineage dependent. In this study, two commonly used chemical fixatives, formaldehyde and methanol, are used for preserving primary mesenchymal stem cells extracted from periodontal ligament, which are valuable cell source for reconstructive dentistry. By means of Raman spectroscopy, cell samples were probed and the impact of these fixatives on their Raman response was analyzed

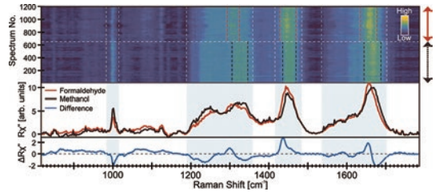

and compared. Different chemical mechanisms are the core processes of formaldehyde and methanol fixation and certain Raman bands are shifted and/or of changed intensity when Raman spectra of cells fixed in that manner are compared. In order to get clearer picture, comprehensive statistical analysis was performed.

Toxicity of Graphene Oxide Against Algae and Cyanobacteria: Nanoblade-Morphology-Induced Mechanical Injury and Self-Protection Mechanism

Malina, T., Maršálková, E., Holá, K., Tuček, J., Scheibe, M., Zbořil, R., & Maršálek, B.
Carbon 2019, 155, 386–396
https://doi.org/10.1016/j.carbon.2019.08.086

Graphene oxide (GO) is the most extensively studied two-dimensional material and has many potential applications in biomedicine, biotechnologies, and environmental technologies. However, its toxicological effects on aquatic organisms have not been properly investigated. Here, we compare the toxicity of differently oxidized graphene oxide systems towards the green alga Raphidocelis subcapitata and the cyanobacterium Synechococcus elongatus. The cyanobacterium exhibited higher GO sensitivity and more rapid growth inhibition than the alga, in keeping with the established antibacterial properties of GO. The toxic effects of GO included shading/aggregation of GOs and nutrient depletion; however a detailed mechanistic study revealed that GO acted against R. subcapitata via an additional, new mechanism. Remarkably, lightly oxidized GO samples induced significantly greater membrane integrity damage than more heavily oxidized GO samples.

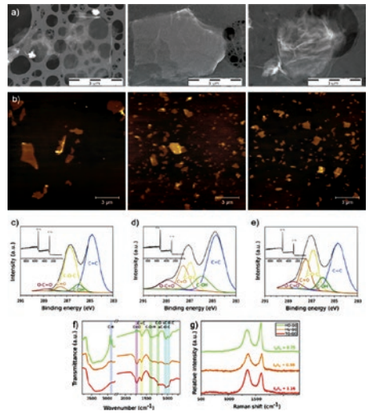

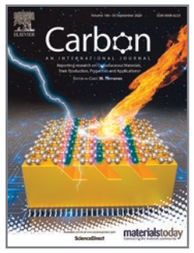

Effect of Grain Boundaries on Charge Transport in CVD-Grown Bilayer Graphene

Wu, J., Li, Y., Pan, D., Jiang, C., Jin, C., Song, F., Wang, G., & Wan, J.
Carbon 2019, 147, 434–440
https://doi.org/10.1016/j.carbon.2019.03.029

Grain boundaries (GBs) in polycrystalline graphene could significantly modulate the physicochemical properties of graphene films, and have attracted intense interest. However, fundamental magnetotransport mechanisms of GBs in bilayer graphene grown by chemical vapour deposition (CVD) are scarcely reported. In this work, we synthesize bilayer graphene bicrystals on polycrystalline Cu foils and measure the electronic properties of such grains as well as of individual graphene grain boundaries. Interestingly, the pronounced metallic character of GB is observed, which is dramatically different from individual grains. Large linear magnetoresistance in graphene bicrystals is observed, which attributes to inhomogeneous charge transport, decorated by quantum interference effects at low temperatures. The measurement data show that individual boundaries between coalesced grains impede electrical transport, suppress the magnetoresistance and

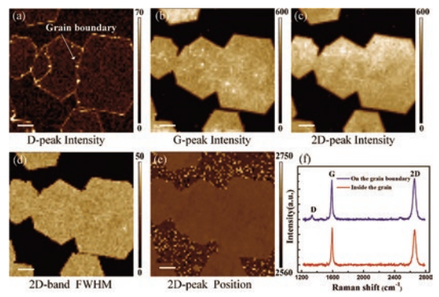

enhance intervalley scattering, leading to degradation of electrical performance of CVD graphene.

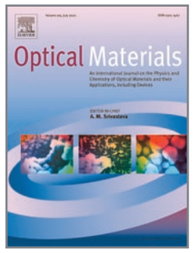

Impact of Composition and Ex-Situ Laser Irradiation on the Structure and Optical Properties of As-S-Based Films Synthesized by PECVD

Nezhdanov, A., Usanov, D., Kudryashov, M., Markelov, A., Trushin, V., De Filpo, G., & Mashin, A.
Optical Materials 2019, 96, 109292
https://doi.org/10.1016/j.optmat.2019.109292

Synthesis of amorphous chalcogenide As-S-based films with arsenic content from 35 to 55 at. % by a PECVD method is achieved. The composition-structure-optical properties relationship is revealed. Varying the composition of the films from $As_{35}S_{65}$ to $As_{55}S_{45}$ is accompanied by a change of the dominant structural units: from $AsS_{3/2}$ pyramids to cage-like As_4S_4 and As_4S_3 units, causing a considerable decrease of the optical band gap from 2.42 to 1.87 eV. It has been found out that modification by a focused laser irradiation (473 nm) leads to formation of micro/nanocrystalline inclusions feasible for applications in medicine, optoelectronics and integrated optics. The type of inclusions depends on the dominant structural units of the initial films. In case of the $As_{55}S_{45}$ film appearance of the dimorphite crystalline phase (α-As_4S_3) is observed. The ex-situ laser modification of the As-S films leads to appearance of a photoluminescence emission,

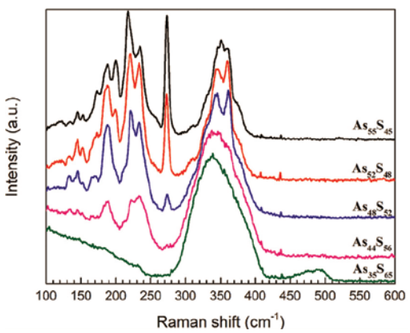

and its maximum position shifts from 1.8 to 2.05 eV depending on the initial film stoichiometry.

Elucidation of an Intrinsic Parameter for Evaluating the Electrical Quality of Graphene Flakes

Lee, H. J., Kim, J. S., Lee, K. Y., Park, K. H., Bae, J. S., Mubarak, M., & Lee, H.
Scientific Reports 2019, 9(1), 1–8
https://doi.org/10.1038/s41598-018-37010-x

A test method for evaluating the quality of graphene flakes, such as reduced graphene oxide (rGO) and graphene nanopowder (GNP), was developed in this study. The pelletizer was selected for a sampling tool, which enables us to formulate the flake sample as a measurable sample. Various parameters were measured from the pelletized sample in order to elucidate the best parameter for representing the quality of the graphene flakes in terms of their electrical properties. Based on the analysis of 4-probe measurement data on the pelletized sample, the best intrinsic parameter is volume resistivity (or volume conductivity) rather than resistivity (or conductivity). Additionally, the possible modification of a sample before and after the pressurization was investigated by electron microscopy and Raman spectroscopy. No significant modification was observed. The volume conductivity in the two types of the graphene was different from their individual conductivities by one order of magnitude.

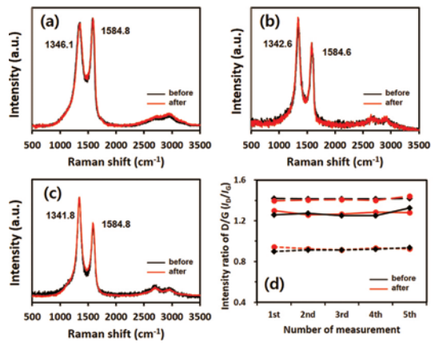

Fabrication of Stacked MoS2 Bilayer with Weak Interlayer Coupling by Reduced Graphene Oxide Spacer

Oh, H. M., Kim, H., Kim, H., & Jeong, M. S.
Scientific Reports 2019, 9(1), 1–7
https://doi.org/10.1038/s41598-019-42446-w

We fabricated the stacked bilayer molybdenum disulfide (MoS_2) by using reduced graphene oxide (rGO) as a spacer for increasing the optoelectronic properties of MoS_2. The rGO can decrease the interlayer coupling between the stacked bilayer MoS_2 and retain the direct band gap property of MoS2. We observed a twofold enhancement of the photoluminescence intensity of the stacked MoS_2 bilayer. In the Raman scattering, we observed that the E^1_{2g} and A_{1g} modes of the stacked bilayer MoS_2 with rGO were further shifted compared to monolayer MoS_2, which is due to the van der Waals (vdW) interaction and the strain effect between the MoS_2 and rGO layers. The findings of this study will expand the applicability of monolayer MoS_2 for high-performance optoelectronic devices by enhancing the optical properties using a vdW spacer.

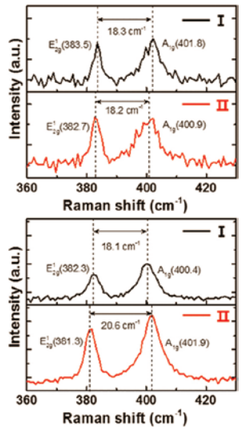

Atomically Dispersed Nickel–Nitrogen–Sulfur Species Anchored on Porous Carbon Nanosheets for Efficient Water Oxidation

Hou, Y., Qiu, M., Kim, M. G., Liu, P., Nam, G., Zhang, T., Zhuang, X., Yang, B., Cho, J., Chen, M., Yuan, C., Lei, L., & Feng, X.
Nature Communications 2019, 10(1), 1–9
https://doi.org/10.1038/s41467-019-09394-5

Developing low-cost electrocatalysts to replace precious Ir-based materials is key for oxygen evolution reaction (OER). Here, we report atomically dispersed nickel coordinated with nitrogen and sulfur species in porous carbon nanosheets as an electrocatalyst exhibiting excellent activity and durability for OER with a low overpotential of 1.51 V at 10 mA cm^{-2} and a small Tafel slope of 45 mV dec^{-1} in alkaline media. Such electrocatalyst represents the best among all reported transition metal-and/or heteroatom-doped carbon electrocatalysts and is even superior to benchmark Ir/C. Theoretical and experimental results demonstrate that the well-dispersed molecular S|NiN$_x$ species act as active sites for catalyzing OER. The atomic structure of S|NiNx centers in the carbon matrix is clearly disclosed by aberration-corrected scanning transmission electron microscopy and synchrotron radiation X-ray absorption spectroscopy together with computational simulations. An integrated photoanode of nanocarbon on a Fe_2O_3 nanosheet array enables highly active solar-driven oxygen production.

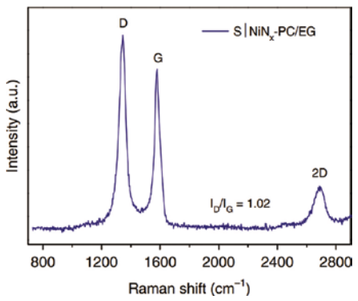

Flow Induced Hela Cell Detachment Kinetics Show that Oxygen-Containing Functional Groups in Graphene Oxide are Potent Cell Adhesion Enhancers

Vlček, J., Lapčík, L., Havrdová, M., Poláková, K., Lapčíková, B., Opletal, T., Froning, J. P., & Otyepka, M.
Nanoscale 2019, 11(7), 3229–3239
https://doi.org/10.1039/c8nr08994a

A broader and quantitative understanding of cell adhesion to two-dimensional carbon-based materials is needed to expand the applications of graphene and graphene oxide (GO) in tissue engineering, prosthetics, biosensing, detection of circulating cancer cells, and (photo)thermal therapy. We therefore studied the detachment kinetics of human cancer cells HeLa adhered on graphene, GO, and glass substrates using stagnation point flow on an impinging jet apparatus. HeLa cells detached easily from graphene at a force of 9.4 nN but adhered very strongly to GO. The presence of hydrophilic functional groups thus apparently enhanced the HeLa cells' adherence to the GO surface. On graphene, smaller HeLa cells adhered more strongly and detached later than cells with larger projected areas, but the opposite behavior was observed on GO. These findings reveal GO to be a suitable platform for detecting cells or establishing contacts, e.g. between graphene-based circuits/ electrodes and tissues. Our experiments also show that the impinging jet method is a powerful tool for studying cellular detachment mechanisms and adhesion strength, and could therefore be very useful for investigating interactions between cells and graphene-based materials.

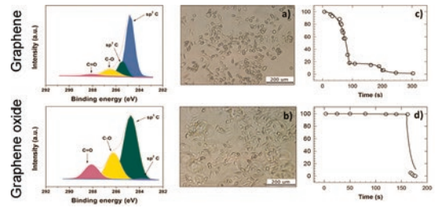

Confocal Raman Microscopy with NTEGRA Spectra

Scientific Digest

Useful Features

Optical Access

NTEGRA Spectra II optical scheme consists of up to three independent channels for sample excitation and signal collection: from top, side and bottom directions. Each optical channel is an independent module and combines with other channels in any configuration. When system is assembled, excitation/collection directions are easily exchanged between each other during less than a minute. Open design provides great opportunities in system customization. Every particular channel allows to observe the sample by the objective with magnification factor up to 100x, excite the sample by laser light and scan by focused laser spot, which is especially important for finding “hot spot” in TERS measurements.

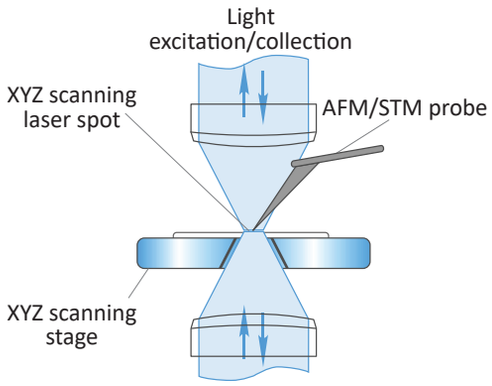

https://www.ntmdt-si.com/products/afm-raman-nano-ir-systems/ntegra-spectra-ii

Fast Scanning - Galvanic Mirror

Fast Raman mapping is a crucial option for high-speed processes detection. Thanks to galvanic scanning mirror technology it is possible to acquire Raman map of selected band with the speed up to 250 Hz, which is about 1 sec/ image. Build-in capacitance sensors make possible laser spot positioning with precision less than 20 nm.

https://www.ntmdt-si.com/products/afm-raman-nano-ir-systems/ntegra-spectra-ii#Ultrafast

Top Visual Probes

TOP VISUAL probes are intended for precise positioning of the tip over the point of interest and for direct real-time observation of sample scanning and modification (nanomanipulation) processes. Also they are suitable for precise positioning of a tightly focused laser spot at the tip apex. This is important for both co-locolaized AFM-Raman mapping and for near-field optical effects between tip and sample (TERS, TEFS, s-SNOM etc). Tips are made of Si and available with coating for conductive measurements or for high reflection in case of IR AFM laser. Both non-contact and contact probes are available.

http://www.ntmdt-tips.com/products/group/vitp